First-Principles Calculations of Structural, Elastic, Electronic, Optical and Thermodynamic Properties of SrSi₂

Md. Atikur Rahman

Department of Physics, University of Rajshahi, Rajshahi 6205, Bangladesh

Abstract: **The structural, elastic, electronic, optical and thermodynamic properties of SrSi₂ at ambient condition have been investigated by using the planewave ultrasoft pseudopotential technique which is based on the first-principles Density Functional Theory (DEF) with Generalized Gradient Approximation (GGA). The optimized lattice parameters, three independent elastic constants (C_{11}, C_{12}, and C_{44}), bulk modulus (B), shear modulus (G), Young's modulus (Y), Pugh's ratio (G/B), Poisson's ratio (v) and elastic anisotropy (A) are estimated and discussed. The electronic structures of SrSi₂ show that the top of the valence band is determined by Si 3p states, the bottom of the conduction band is determined by Sr 3d states, and the band structure presents an indirect narrow-gap semiconductor character with energy gap of 0.059 eV. Finally, the thermodynamic properties and the different optical properties such as, dielectric function, absorption, loss function, conductivity, reflectivity and refractive index of SrSi₂ are obtained and discussed in detail.**

Keywords: **SrSi₂; Ab initio calculations; Structural, Elastic, Electronic, Optical and Thermodynamic Properties**

1. INTRODUCTION

Silicon is a chemical element with symbol Si and atomic number 14. It is a tetravalent metalloid, less reactive than its chemical analog carbon, the nonmetal directly above it in the periodic table, but more reactive than germanium, the metalloid directly below it in the table. Controversy about silicon's character dates to its discovery; it was first prepared and characterized in pure form in 1823. In 1808, it was given the name silicium (from Latin: *silex*, hard stone or flint), with an -ium word-ending to suggest a metal, a name which the element retains in several non-English languages. However, its final English name, first suggested in 1817, reflects the more physically similar elements carbon and boron. Silicon is the eighth most common element in the universe by mass, but very rarely occurs as the pure free element in nature. It is most widely distributed in dusts, sands, planetoids, and planets as various forms of silicon dioxide (silica) or silicates. Over 90% of the Earth's crust is composed of silicate minerals, making silicon the second most abundant element in the Earth's crust (about 28% by mass) after oxygen . Silicon is a primary material in modern solid-state electronics and semiconducting silicides which are composed of non- or less toxic and naturally abundant elements from earth's crust have attracted considerable attention because of their practical applications in photoelectric and thermoelectric [1-3] devices, such as light-emitting diode. Thermoelectric materials are capable of converting waste heat into electricity [4]. It is very important for developing alternative energy technologies in the reduction in our dependence on fossil fuels [5] to utilize the technology of energy conversion. The effectiveness of a material for thermoelectric applications is determined by the dimensionless figure of merit, $ZT=S^2\sigma T/k$, where S is the Seebeck co-efficient, σ the electrical conductivity, k the thermal conductivity and T the absolute temperature [6]. Photoelectric devices give an electrical signal in response to visible, infrared, or ultraviolet radiation. They are often used in systems which sense objects or encoded data by a change in transmitted or reflected light. Photoelectric devices which generate a voltage can be used as solar cells to produce useful electric power. The operation of photoelectric devices is based on any of the several photoelectric effects in which the absorption of light quanta liberates electrons in or from the absorbing material. Photoconductive devices are photoelectric devices which utilize the photo-induced change in electrical conductivity to provide an electrical signal. Among alkaline-earth metals disilicides, very recently SrSi₂ was reported to be a narrow-gap

semiconductor with a band gap of 0.035 eV estimated by the Hall coefficient measurements ranging from 10 to 300 K and the electrical resistivity measurements ranging from 2 to 760 K [7]. Narrow gap semiconductors are semiconducting materials with a band gap that is comparatively small compared to silicon. They are used as infrared detectors or thermoelectric. On the other hand, band structure calculations [8-12] indicated the presence of a semimetallic character, while different calculations show them to be metallic [13-14]. Therefore, electrical properties of $SrSi_2$ are still unclear, further investigation is necessary to clarify its electrical properties. Based on above, in this work, structural, elastic, electronic, optical, and thermodynamics properties of $SrSi_2$ have been investigated by using the first-principles density function calculations in order to reveal a complete understanding of the basically physical properties of $SrSi_2$ and the results are analyzed in detail. The rest of the paper is organized as follows: in Sec. 2, description of the method of calculation is given; Sec. 3 contains our results and discussion, involving structural, elastic, electronic, optical and thermodynamic properties for $SrSi_2$ composition. Finally, the conclusion is given in Sec.4.

2.   COMPUTATIONAL METHODS

The present calculations of various properties of $SrSi_2$ have been investigated upon *ab-initio* techniques. The electronic structures of $SrSi_2$ have been computed using the ultrasoft pseudopotential (PWPP) method (CASTEP Code [15]). All the calculating properties for $SrSi_2$ ($P4_332$), we used   8x8x8 Monkhorst-pack [16] grid, a plane wave basis set cut-off energy of 350 eV and default the Perdew-Burker-Ernzerhof and generalized gradient approximation (GGA) density function (DF). In CASTEP code, we have used the ultrasoft pseudopotential for Sr and Si. As the name suggests, ultrasoft pseudopotential attain much smoother (softer) pseudo-wavefunctions so use considerably fewer plane waves for calculations of the same accuracy. The kinetic energy cutoff controls number of plane waves at given k-point. This is the single parameter which can have an enormous effect on the quality of the calculation. Basically, the calculation is better converged due to the higher energy cut-off. For all first-principles calculations, we must pay attention to two convergence issues, i.e. one is the energy cut-off, which is the cut-off for wave-function expansion and the other is number of k- points, which measures how well our discrete grid has approximated the continuous integral.

3.   RESULTS AND DISCUSSION

3.1 Structural and elastic properties of $SrSi_2$:

At atmospheric pressure and room temperature, $SrSi_2$ crystallizes in the cubic structure with space group $P4_332$. The corresponding number of group is 212[17] and three atoms in one unit cell. Fig.1 shows the perspective views of the $SrSi_2$ structure. It contains four Sr atoms and eight Si atoms, each Si atom is surrounded by three Si atoms and seven Sr atoms, and each Sr atom is surrounded by fourteen Si atoms and six Sr atoms. Fig.1 shows the schematic representation of the unit cell of $SrSi_2$ and some neighbor atoms in cell. The nearest-neighbor <Si-Si> distances are 2.402 Å, and <Si-Sr> distances are 3.252 Å, which are excellent agreement with the experimental value of 2.39 Å and 3.25 Å respectively [18-19].The nearest neighbor distances of $SrSi_2$ are shown in Table 1.

Table 1: Nearest neighbor distances (Å) of $SrSi_2$ structure

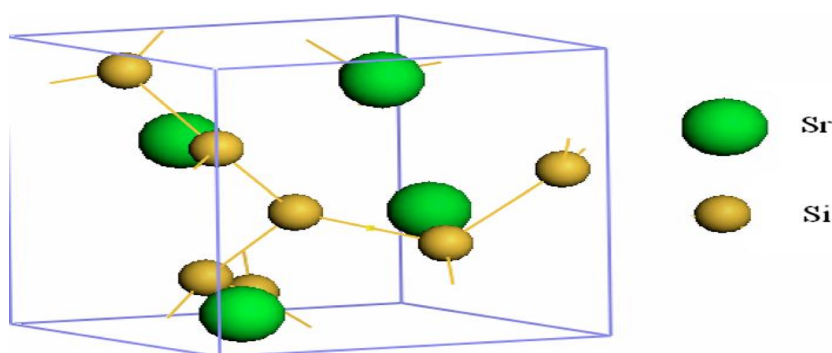| Nearest neighbor atom	$SrSi_2$
Si- Si	2.402
Si- Sr	3.252

Fig. 1: The cubic crystal structure of $SrSi_2$

The geometry optimization was carried out as a function of the normal stress by minimizing the total energy for the compound $SrSi_2$. The procedures lead to successful optimization of the $SrSi_2$ structure. For $SrSi_2$, our calculated value of the lattice constant (6.556 Å) is in good agreement with experimental value, [18]. The optimized lattice parameters and volume of $SrSi_2$ at zero pressure are shown in Table 2 (CASTEP code). These results are in good agreement with the available theoretical and experimental data [17-19]

Table 2: Lattice parameters and atomic coordinates for $SrSi_2$

System	Phase	Lattice parameters (Å)	Atomic coordinates
Cubic	$SrSi_2$	$a=b=c$=6.556, 6.545a $\alpha=\beta=\gamma$=90	Sr: 4a(0.125, 0.125, 0.125) Si: 8c(0.423, 0.423, 0.423)

. ªExpt.[17].

Elastic properties of a solid are important because they relate to various fundamental solid-state phenomena such as interatomic bonding equations of state and phonon spectra. Elastic properties are also linked thermodynamically with specific heat, thermal expansion and Debye temperature, most importantly, knowledge of elastic constants is essential for many practical applications related to the mechanical properties op a solid such as load deflection, thermo-elastic stress, internal strain, sound velocities and fractural toughness.

The knowledge of the elastic properties of $SrSi_2$ compound will be great interest in understanding its behavior. Elastic properties of single cubic crystal can be described using three independent elastic moduli C_{11}, C_{12} and C_{44} is related to the unidirectional along the principal crystallographic directions, while C_{44} reflects the resistance to share deformation [20]. Our calculated values of C_{11}, C_{12} and C_{44} are listed in Table 3. Further information about the stability of system can be achieved from the elastic moduli values, at zero pressure for cubic symmetry the stability the criterion are given by

$C_{44}> 0$, $C_{11}>\left|C_{12}\right|$, $C_{11}+2C_{12}> 0$

These conditions are satisfied by the values reported in Table 3.

Table 3: Single Crystal Elastic Constants (C_{ij} in GPa).

Compound	C_{11}	C_{44}	C_{12}
$SrSi_2$	84.79	44.92	42.59

Polycrystalline elastic constants are more attractive in technological characterizations of materials, to obtain such quantities ; we have used the Reuss assumption to estimate the bulk modulus B, shear modulus G, Young modulus Y, Poisson ratio υ, and anisotropy factor A, according to the following relations:

B= ($C11$ +2$C12$) / 3 (1.1)

G = 5($C11$-$C12$) $C44$/ (4$C44$+3($C11$-$C12$)) (1.2)

Y = 9BG / (3B+G) (1.3)

υ = (3B-2G)/ 2 (3B+G) (1.4)

A = 2$C44$/ ($C11$-$C12$) (1.5)

The calculated bulk modulus B, shear modulus G, Young's modulus Y, Poisson ratio υ and anisotropy factor A of $SrSi_2$ compound are given in Table 4. The Young's modulus, also known as the tensile modulus Y, is defined as the ratio between stress and strain and used to provide a measure of stiffness, i.e., the larger the value of Y, the stiffer the material. From our calculation, we have the value of Y for $SrSi_2$ is 53.63 GPa. So we conclude that this is a stiff material. A simple Relationship, which empirically links the plastic properties of materials with their elastic moduli, was proposed by Pugh [22]. The shear modulus G represents the resistance to plastic deformation while B represents their resistant to fracture [22]. If G/B<0.5 the material will behave in a ductile manner, and vice versa, if G/B>0.5 the material demonstrates brittleness. In our case, we have found that G/B ratio is 0.57, classifying this material as brittle. An additional argument for the variation in the brittle/ductile behavior of SrSi2 phase follows from the calculated Poisson's ratio υ, Table 4. Indeed, for brittle materials these values are small enough, whereas for ductile metallic materials υ is typically 0.33[23]. In our case, the obtained value of υ is 0.258 which indicates that the examined compound belongs to brittle material.

Table 4: Polycrystalline elastic constants.

Compound	*B* (GPa)	*G* (GPa)	*Y*(GPa)	*v*	*A*	*G/B*
SrSi$_2$	58.21	33.53	53.67	0.258	2.41	0.57
SrSi$_2$	50.30[b]					

[b]Ref. [24]

Elastic anisotropy of crystals is a very important factor for material science of SCs, since it correlates with the possibility of appearance of microcracks in these materials [25, 26].The anisotropy factor *A* provides a measure of the degree of anisotropy in the bonding in the different planes. For an isotropy crystal, the value of *A* should be equal to the unity, while any deviation from the unity is a measure of the degree of elastic anisotropy possessed by the crystal [24]. Our estimations (Table 4) demonstrate that the examined compound SrSi$_2$ is an anisotropic.

3.2 Electronic and optical properties of SrSi$_2$:

The electronic band structure is the spectrum of the energy eigen values of a periodic system. The band structure diagram contains information about both the bonding interactions. However, the ability to understand the band structure diagram allows one to extract valuable information about a material: electronic conductivity, optical properties and stability of compound toward oxidation or reduction. In this way knowledge of the electronic band structure provides predictive insight and understanding of certain very important physical properties of solids. The energy band structures with the geometrically optimized structure are calculated for SrSi$_2$ along the high symmetry directions in the BZ, as shown in Fig. 2. The total density of states (TDOS) and the partial density of states (PDOS) are also plotted in Fig.3. For SrSi$_2$, the top of the valence band (VB) is mainly composed of Si 3p state. The bottom of conduction band (CB) is dominated by Sr 3d state. At the same time, it is obvious that there is a strong hybridization between the Si 3s and the 3p states (Fig.3), which facilitates the formation of covalently bonded three-dimensional Si anionic network in the crystal. The result is consistent with the previous study [11, 12] .The Fermi level E_F is located in the narrow dip of the DOS curve, the band structure of SrSi$_2$ shows that top of the valence band is located between G and R. The energy minimum of the lowest conduction band is located between G and M (Fig. 2). So SrSi$_2$ presents an indirect narrow gap semiconductor, which is an excellent agreement with experimental determination by Emai et al [27, 28]. The energy gap 0.059 eV is little higher than the observed value of 0.035 [29] and 0.0437 [30]. This is because of the fact that we make use of the GGA to the exchange-correlation part of the potential which overestimates the band gap value in most semiconductor and insulators. As is clearly seen, some theoretical calculations predict that SrSi$_2$ is a semimetal [8–12] or metal [13, 14] materials, which is inconsistent with experimental observation [7].
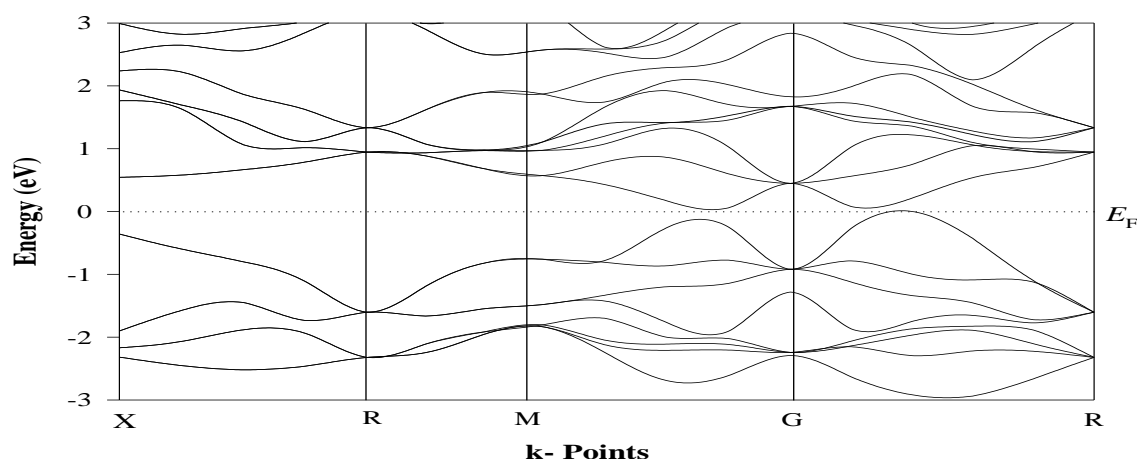

Fig. 2: Band structure of SrSi$_2$. The position of the Fermi level is set to be at 0 eV.

In solid-state and condensed matter physics, the density of states (DOS) of a system describes the number of states per interval of energy at each energy level that are available to be occupied. A high DOS at a specific energy level means that there are many states available for occupation. A DOS of zero means that no states can be occupied at that energy level.

The total density of states is written as a sum over atomic contributions. The density of states is calculated by using the following expression

$$n(\epsilon) = 2 \sum_{n,k} \delta\left(\epsilon - \epsilon_n^k\right) = (2/V_{BZ}) \sum_n \int \delta(\epsilon - \epsilon_n^k)\, dk$$

and the number of electron in the unit cell is given by

$$\int_{-\infty}^{\epsilon_F} n(\epsilon)\, d(\epsilon)$$

The total and partial electronic densities of states of SrSi$_2$ at ambient pressure are illustrated in Fig.3 where the vertical line indicates the Fermi level E_F. The partial contributions of s, p and d orbitals at E_F of Sr and Si are displayed. In Fig. 3 the conduction band above the Fermi level is mostly derived from the Sr states. Note that, the most remarkable feature of the DOS for this compound is a narrow intense peak in the vicinity of the Fermi level. The calculated values of partial and DOS at the Fermi level show that dominating contributions are due to Sr d states, where as the contribution of the states of Si is much less. The partial contributions of s, p and d orbitals at E_F of Sr and Si are also displayed. The total and partial densities of states of SrSi$_2$ are given in Table 5.

Table 5: Total and partial DOS of SrSi$_2$

Compound	pressure (GPa)	Partial densities of states (PDOS) (electrons/ eV)					Total DOS (electrons/ eV)
		Sr- s	Sr- p	Sr- d	Si- s	Si- p	
SrSi$_2$	0	0.311	0.000	0.499	0.242	1.472	2.526
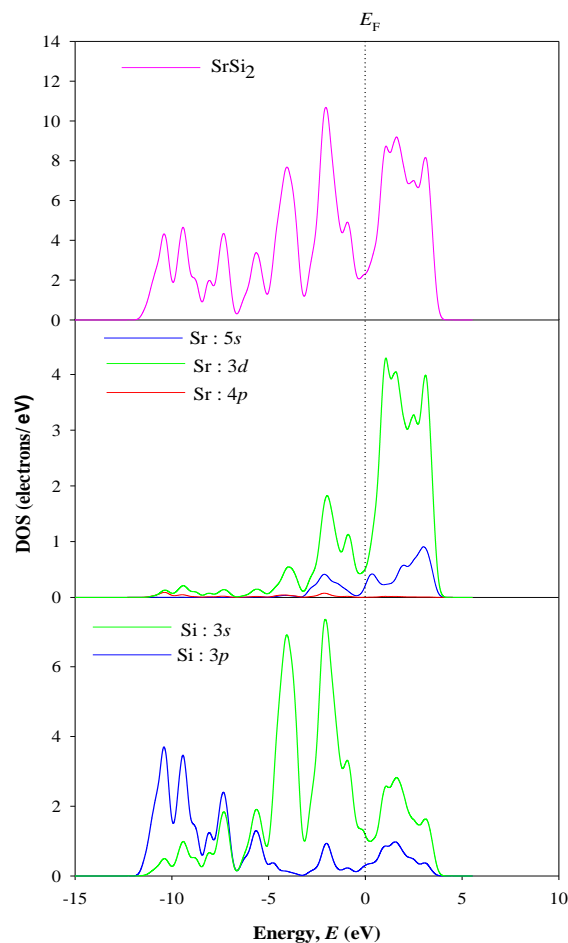
Fig. 3: Total and partial densities of states of SrSi$_2$ at ambient pressure.

Optical Properties:

The study of the optical functions helps to give a better understanding of the electronic structure. Here the optical properties such as complex dielectric function $\varepsilon(\omega)$, complex conductivity $\sigma(\omega)$, refractive index, reflectivity, absorption coefficient and loss function of $SrSi_2$ are calculated. We have used a 0.5 eV Gaussian smearing for all calculations. The calculated optical properties at the equilibrium lattice constants are presented in Figs. 4 and 5.

The dielectric function of $SrSi_2$:

The dielectric function is an important parameter for a material, because it is the fundamental feature of the linear response to an electromagnetic wave, and determines uniquely the propagation behavior within the radiation. In order to improve our understanding of the optical spectra, it is necessary to determine the k points locations of the interband transitions which correspond to the main peaks in the imaginary part of the dielectric function. The calculated dielectric function of $SrSi_2$ is shown in Fig. 4(a). The peaks of the imaginary part of dielectric function are related to the electron excitation. The imaginary part $\varepsilon_2(\omega)$ exhibit the maximum peak at 2.08 eV. For the real part $\varepsilon_1(\omega)$ spectra minimum at about 4.79 eV. The calculated static dielectric constant, $\varepsilon_1(0)$ is 26.85, suggested that, $SrSi_2$ is a dielectric material.

Absorption coefficient of $SrSi_2$:

The dielectric function and absorption coefficient are derived from $\propto(\omega) = \omega\,\varepsilon_2(\omega)/ne$, Fig. 4(b) shows the curve of the absorption coefficient. Two main absorption peaks are observed at 5.11eV and 20.52 eV, which are ascribed to interband transition between Sr $3d$ states at the conduction band (CB) and Si $3P$ in the valence band (VB) states. When the photon energy is below 0.11 eV and above 22.50 eV, $SrSi_2$ is transparent. For first absorption peak, the absorption coefficient increases from 1.05 eV to 5.11 eV, it reaches the maximum value 2.2×10^5 cm^{-1} at 5.11 eV and then decreases with the increasing of photon energy till zero and 14.17 eV. For second absorption peak, the absorption coefficient increases from 17.29 eV to 20.52 eV, it reaches the maximum value 1.41×10^5 cm^{-1} at 22.52 eV and then decreases with increasing of photon energy till zero, and 22.61 eV corresponds to the value of indirect band gap.

Loss function of $SrSi_2$:

In Fig.4(c) we show the electron energy loss function $L(\omega)$. $L(\omega)$ is an important parameter describing the energy loss of a fast electron traversing in a material and usually large at the plasma energy. The peaks in $L(\omega)$ spectra represent the characteristic associated with the plasma resonance and the corresponding frequency is the so-called plasma frequency ω_p. In the energy-loss spectrum, we see that the plasma frequency ω_p is 11.98 eV for $SrSi_2$ structure, which corresponds to a rapid reduction in the reflectance. This process is associated with the transitions from the filled Si $3p$ bands to empty CB.

The conductivity of $SrSi_2$:

The photoconductivity $\sigma(\omega)$, which is directly related to the energy band structure of solids. In Fig. 5(a) photoconductivity starts with photon energy 0.47 eV. This shows that the material has a band gap of about 0.47 eV. The real part of the conductivity is zero below 0.24 eV and above 22.37 eV. Moreover, the photoconductivity and hence electrical conductivity of a material increases as a result of absorbing photons. The photons must have energy sufficient enough to overcome the band gap in the material.

The reflectivity of $SrSi_2$:

The reflectivity can be expressed by $n_1=1$, $n_2= n+ ik$. The reflectivity is derived from $R(\omega)= [(n-1)^2+k^2]/[(n+1)^2 + k^2]$. Fig. 5(b) shows the reflectivity of $SrSi_2$. From the reflectivity spectrum it can be seen that large reflectivity is obtained in the low-energy region, which is the characteristics of high conductance.

The refractive index of $SrSi_2$:

The refractive index n and extinction coefficient k are derived from $n^2-k^2= \varepsilon_1$. $2nk = \varepsilon_2$. The refractive index is shown 5(c). The static refractive index n_0 is 5.05. The real part of the refractive index reaches a maximum value of 5.34 at 1.17 eV and then reduces sharply.
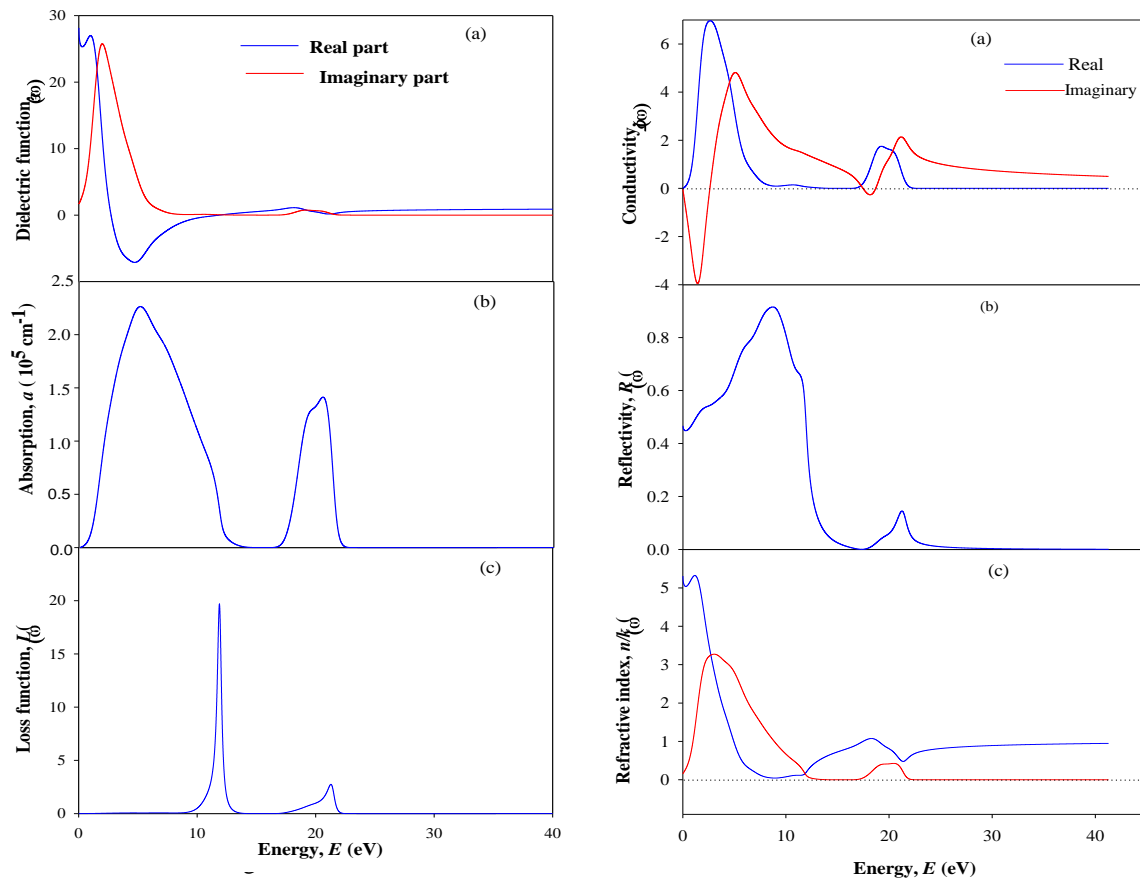
Fig.4: Optical functions of SrSi$_2$ (a) the dielectric function, (b) absorption spectrum and (c) energy-loss function and Fig. 5: (a) conductivity, (b) reflectivity and (c) refractive index.

3.3 Thermodynamic properties

The temperature at which all the phonon vibrations have the same frequency is called the Debye temperature. n Debye theory, the Debye temperature θ_D is the temperature of a crystal's highest normal mode of vibration, i.e., the highest temperature that can be achieved due to a single normal vibration. The Debye temperature is given by

$$\theta_D = \frac{h\nu_m}{k},$$

Where h is Planck's constant, k is Boltzmann's constant, and νm is the Debye frequency.

The concept of the Debye temperature, has played an important role in the field of thermophysical properties of materials ever since its introduction. It is basically a measure of the vibrational response of the material and, therefore, intimately connected with properties like the specific heat, thermal expansion, and vibrational entropy [31]. The Debye temperature is not a strictly determined parameter; various estimates may be obtained through well established empirical or semi empirical formulae, relating θ_D with various macroscopic properties [32]. The values of Debye temperature have been obtained from the knowledge of the elastic constants and the sound velocities (including longitudinal, shear, and average wave velocities) by using the standard tables for C_v /3R versus θ_D/T [33]. Our calculated Debye temperature is presented in Fig. 6. The value thus obtained is 408 K, which is in good agreement with the other theoretical value of 380K [9].There is no experimental data for the comparison. In order to calculate the temperature dependence of the specific heat we need the phonon DOS, which can be obtained by standard procedures from the phonon-dispersion relations of Fig. 7. We display in Fig.8 the total PDOS calculated for SrSi$_2$, together with the separate contributions of the Sr and Si vibrations. The figure indicates that the phonon structure is stable since throughout the BZ all phonon frequencies are positive. It is also found that there are two phonon bands with frequencies below about 300 cm^{-1} and frequencies between 300 and 400 cm^{-1}. The frequency gaps are about 7 cm^{-1}. The highest phonon frequency is 384 cm^{-1}. From Fig. 8, we can find that the low-frequency band below 150 cm^{-1} is dominated by motion of the Sr ions and the high-frequency band above 150 cm^{-1} is mainly being ascribed to the Si ions. According to point group theory, optical modes are triple degenerate at the zone-center, which agrees rather well with our results.
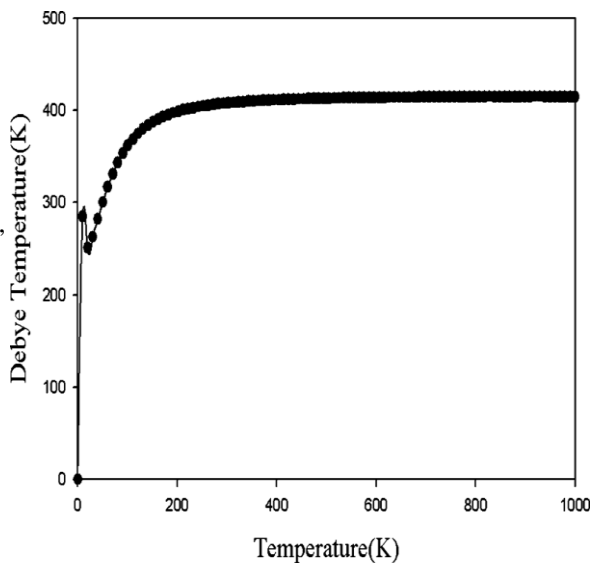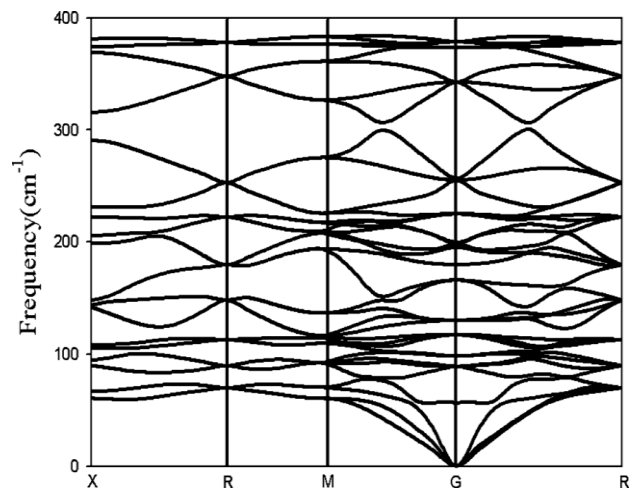
Fig. 6: The Debye temperature relations of SrSi$_2$.   **Fig. 7: Phonon-dispersion relations of SrSi$_2$.**
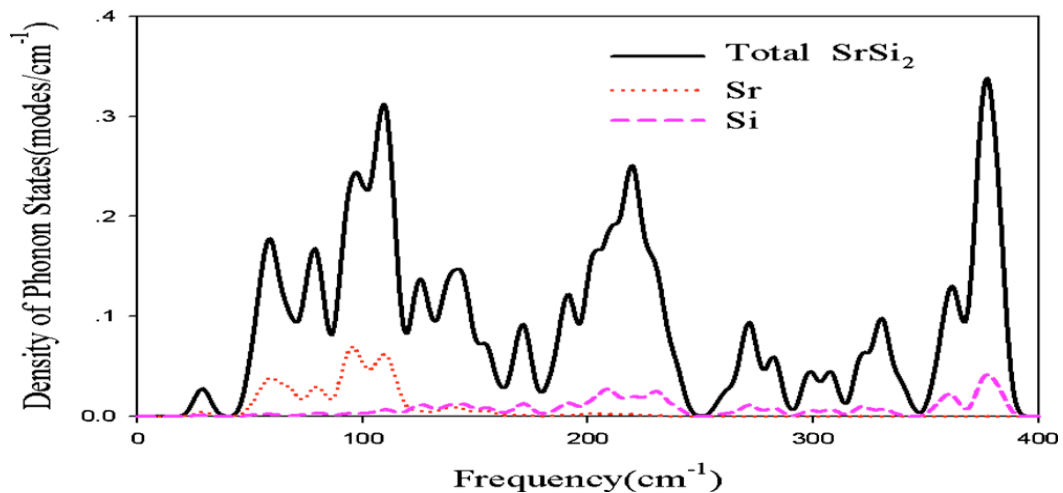

Fig. 8: PDOS of SrSi$_2$ obtained from the dispersion relations shown in Fig. 7.

Once the phonon spectrum over the entire BZ is obtained, the thermodynamic functions of SrSi$_2$ can be determined by the entire phonon spectrum, assuming that the vibrational degrees of freedom of the lattice play a noticeable role while the electronic degrees of freedom are ignorable. In the present work, the phonon contribution to the Helmholtz free energy F, the phonon contribution to the enthalpy H, the entropy S, and the constant-volume specific heat C_v, at temperature T are calculated using the formulas in Ref. 34 within the harmonic approximation, shown in Fig. 8.Δ F and ΔE at zero-temperature represent the zero-point motion, which can be calculated from the expression as $\Delta F = \Delta E_0 = 3nN \int_0^{\omega max} (\frac{\hbar\omega}{2}) g(w) dw$

where n is the number of atoms per unit cell, N is the number of unit cells, w is the phonon frequencies, w_{max} is the largest phonon frequency, and $g(w)$ is the normalized PDOS with $\int_0^{\omega max} (\frac{\hbar\omega}{2}) g(w) dw = 1$

The calculated zero temperature values do not vanish due to the zero-point motion, which are $\Delta F_0 = \Delta E_0 = 0.441$ eV for SrSi$_2$. When the temperature increases, the calculated ΔF decrease gradually; the calculated H and S increase continually, and the calculated constant-volume specific heat C_v tend to the asymptotic limit of $C_v = 3nNk_B = 70.9$ Cal/Cell K, as are shown in Fig. 9. Above 400 K, the $C_v(T)$ data approximately linear in T, which can be attributed to the thermal expansion. The experimental thermodynamic data cannot be found; therefore it is difficult to evaluate the magnitude of errors between theory and experiments. Our calculated results have been shown as a prediction for future investigations.
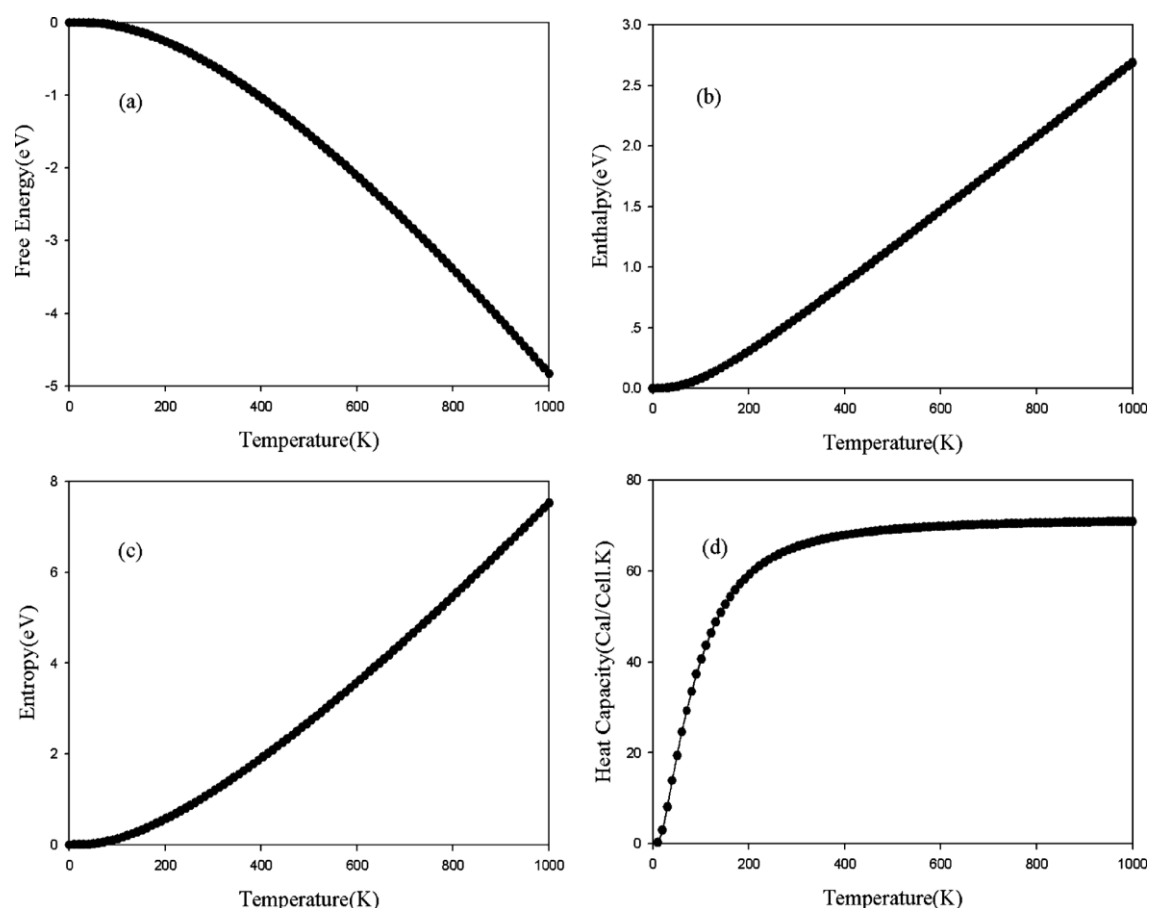
Fig. 9: The calculated phonon contribution to the Helmholtz free energy ΔF (a), the enthalpy H (b), the entropy S (c), and the constant-volume specific heat C_v (d) of SrSi$_2$.

4.   CONCLUSION

Employing the pseudopotential planewave (PP-PW) approach based on density functional theory (DFT), with generalized gradient approximation (GGA), we have studied the structural, elastic, electronic, optical and thermodynamic properties of SrSi$_2$ at ambient condition. Our structural parameters of SrSi$_2$ are in good agreement with the experimental data. Furthermore, the Si–Si bond shows covalent character. The electronic structures show that the top of the VB is determined by Si $3p$ states, the bottom of the CB is determined by Sr $3d$ states, and the band structure presents an indirect narrow-gap semiconductor with energy gap of 0.059 eV, which is in excellent agreement with experimental determination. The evaluated elastic parameters allow us to conclude that SrSi$_2$ phase is mechanically stable. The small value of bulk modulus indicates that the material is soft. The obtained Poisson's ratio value indicates that this material possesses brittle behavior. The dielectric function, absorption spectrum and energy-loss function, conductivity, reflectivity and refractive index are obtained and discussed in detail. It is shown that SrSi$_2$ is a promising dielectric material. The absorption for the ray focuses on ultraviolet light regions. We also observe that the photoconductivity and hence the electrical conductivity of the material increases as a result of absorbing photons. Finally, using the calculated PDOS, the thermodynamic properties are determined with the harmonic approximation.

REFERENCES

[1]   T. . Tritt, M. Kanatzidis, H. B. Lyon, Jr., and G. Mahan, Symposium Proceedings of the Materials Research Society (Materials Research Society, Pittsburgh, 1997), P. 478.

[2]   C. S. Lue, Y.-K. Kuo, C. L. Huang, and W. J. Lai, Phys. Rev. B **69**, 125111(2004).

[3]   Y. K. Kuo, K. M. Sivakumar, S. J. Huang, and C. S. Lue, J. Appl. Phys.**98**, 123510 (2005).

[4]   T. M. Tritt, Science **283**, 804 (1999).

[5]   T. M. Tritt and M. A. Subramanian, MRS Bull. **31**, 188 (2006).

[6]   *CRC Handbook of Thermoelectrics*, edited by D. M. Rowe CRC Press, New York,(1995).

[7]   M. Imai, T. Naka, T. Furubayashi, H. Abe, T. Nakama, and K. Yagasaki, Appl. Phys. Lett. **86**, 032102 (2005).

[8]   B. Hammer, L. B. Hansen, and J. K. Norskov, Phys. Rev. B **59**, 7413 (1999).

[9]   K. Hashimoto, K. Kurosaki, Y. Imamura, H. Muta, and S. Yamanaka, J. Appl. Phys. **102**, 063703 (2007).

[10]   J. Evers, J. Solid State Chem. **24**, 199 (1978).

[11]   Y. Imai and A. Watanabe, Intermetallics **14**, 666 (2006).

[12]   S. Brutti, D. N. Manh, and D. G. Pettifor, Intermetallics **14**, 1472 (2006).

[13]   Y. Imai and A. Watanabe, Intermetallics **10**, 333 (2002).

[14]   J. Evers and A. Weiss, Mater. Res. Bull. **9**, 549 (1974).

[15]   I.R. Shein, V.V. Bannikov, A.L. Ivanovskii, Physica C 468 (2008) 1.

[16]   D. Vanderbilt, Phys. Rev. B 41, 7892 (1990).

[17]   K. Hashimoto, K. Kurosaki, Y. Imamura, H. Muta, and SYamanaka, J.Appl. Phys. 102, 063703 (2007).

[18]   J. Evers, J. Solid State Chem. 24, 199 (1978).

[19]   Y. Imai, A. Watanable, Thin Solid Films 515 (2007) 8219.

[20]   S.F. Pugh, Philos. Mag. 45 (1954) 823.

[21]   G. Vaitheeswaran, V. Kanchana, R.S. Kumar, A.L. Cornelius. M.F. Nicol, A. Savane, A. Delin, B. Johansson. Phys. Rev. 75 (2007) 014107.

[22]   J. Haines, J. Leger, G. Bocquillon, Ann. Rev. Mater. Res. 31 (2001) 1.

[23]   E.O. Chi, W.S. Kim, N.H. Hur, D. Jung, Solid State Communications121 (2002) 309-312.

[24]   P. Ravindran, L. Fast, P. A. Korzhavyi, B. Johnnsson, J.Wills, and O. Eriksson, J.Appl.Phys.84, 4891 (1998).

[25]   V. Tvergaard and J. W. Hutchinson, J. Am. Chem. Soc.71,157 (1998).

[26]   M. Imai, T. Naka, T. Furubayashi, H. Abe, T. Nakama, and K.Yagasaki, Appl. Phys. Lett. 86, 032102 (2005).

[27]   M. Imai, T. Naka, H. Abe, and T. Furubayashi, Intermetallics 15, 956 (2007).

[28]   G. Vaitheeswaran, V. Kanchana, R.S. Kumar, A.L. Cornelius. M.F.   Nicol, A. Savane, A. Delin, B. Johansson. Phys. Rev. 75 (2007) 014107.

[29]   E.O. Chi, W.S. Kim, N.H. Hur, D. Jung, Solid State Communications 121 (2002) 309-312.

[30]   G. Grimvall, Thermophysical Properties of Materials (North Holland, Amsterdam, 1956).

[31]   H. M. Leadbetter, in Elastic Properties of Materials at Low Temperatures, edited by R. P. Reep and A. F. Clark (ASM Metal Park, Ohio, 1983).

[32]   G. K. Ghatak and L. S. Kothari, An Introduction to Lattice Dynamics (Addison Wesley Pub. Co., USA, 1972).

[33]   C. Lee and X. Gonze, Phys. Rev. B **51**, 8610 (1995).